

Modulation of Iron Catalytic Activity to Dopamine Oxidation through Additional Iron Ligation

Ming La*, Chang-Dong Chen, He Li, Cheng-Ye Yang

College of Chemistry and Chemical Engineering, Pingdingshan University, Pingdingshan, Henan 467000, People's Republic of China

*E-mail: mingla2011@163.com

Received: 2 August 2014 / Accepted: 31 August 2014 / Published: 29 September 2014

Parkinson's disease (PD) is characterized by the selective degeneration of dopaminergic cells. This bodes well for the role of dopamine (DA) in the etiology of PD, possibly through the Fe(III) catalyzed production of DA derived neuronal toxins. We investigated how the presence of iron ligation of nitrilotriacetic acid (NTA, a well known tetradentate ligand) affected the catalytic oxidation reaction by electrochemistry and UV-vis spectrophotometer. A relatively stable DA-Fe(III)-NTA ternary complex is identified. The additional ligation by NTA shifted the catecholate-Fe(III) ligand metal charge transfer (LMCT) band to a longer wavelength and caused the change of the redox potentials of both DA and Fe(III) center in the ternary complex. Fe(III)-catalyzed DA oxidation kinetics in the absence and presence of NTA was also studied. Remarkably, the additional ligation by NTA was found to totally reverse the Fe(III) catalytic effect. NTA as a tetradentate ligand together with DA saturates all coordination sites of Fe(III). The inaccessibility of O₂ to the metal center blocks the Fe(III) bridged electron transfer between O₂ and DA. Our findings have a significant biological implication.

Keywords: dopamine; iron; electrochemistry; nitrilotriacetic acid; catalytic activity; hydrogen peroxide

1. INTRODUCTION

As one of the most common neurodegenerative diseases, Parkinson's disease (PD) is accompanied by the degeneration of neuromelanin-containing dopaminergic neurons in the substantia nigra (SN) zona compacta which produces the neurotransmitter of dopamine (DA) [1]. The molecular mechanism responsible for PD is still unknown although oxidative stress resulted from the reactive oxygen species (ROS) has been definitely recognized as a pathogenetic factor that induces the formation of protein inclusions and selective degeneration and further leads to excitotoxicity and

mitochondrial dysfunction [2]. DA is a member of neurotransmitter of the catecholamine family [3]. It has been well-established that DA was first synthesized in the cytoplasm and then sequestered rapidly by the vesicular monoamine transporter back into presynaptic vesicles where it was stabilized at low pH [4, 5]. When the amount of cytosolic DA exceeds the physiological level, DA can be metabolized via monoamine oxidase and aldehyde dehydrogenase into the non-toxic metabolite [6] or it can be sequestered into cytosol [7] where it undergoes auto-oxidation to form a dark polymer neuromelanin (NM). NM is mainly distributed in the dopaminergic neurons of SN and the noradrenergic neurons of the locus coeruleus [8]. It has been proven that a number of DA oxidation intermediates (e.g. 6-hydroxydopamine or 6-OHDAQ) are neurotoxic [9]. Depending on how DA is oxidized, the kinetics for its oxidation and the yields of different intermediates vary [10]. Therefore, it is vital to understand what influence the oxidation kinetics and its oxidation pathways.

Iron acquisition is a fundamental process in almost all living organisms (e.g. O₂ transport, DNA synthesis and electron transport) [11]. The redox active iron is also a potential toxin, so is highly regulated and usually stored in the redox inactive mineral form encapsulated by intracellular ferritin. However, the disruption of iron homeostasis is evidenced in most of the neurodegenerative diseases. In PD, compared with age-matched disease-free subjects, the total concentration of iron in the parkinsonian SN has been significantly increased [12]. Interestingly, via biochemical and in vivo brain imaging techniques, the increased level of iron was found to restrict the SN pars compacta in the ferric form and coordinate to the phenolic oxygen of NM [12, 13]. It is therefore supposed that the excess iron may act as an endotoxin that mediates SN cell death in PD by catalyzing the formation of hydroxyl radical (OH•) from H₂O₂ and superoxide anion radical (O₂•) [12].

Due to the high affinity of catecholate analogues to Fe(III), the colored catecholate-iron(III) complex has been extensively investigated and characterized by spectrophotometric and electrochemical assays [14-22]. Among them, one of typical examples is concerned with the oxidative cleavage reaction of catechol derivatives catalyzed by intradiol catechol dioxygenases [14]. The intradiol enzyme, which contains an Fe(III) center, cleaves a C-C bond between two hydroxyl groups of the catechol substrates. However, differing from catechol, DA undergoes more complicated oxidation reactions [15]. It is generally accepted that the DA-Fe(III) complex could slowly fade due to the internal electron transfer reaction [15, 23, 24]. In the complex, the partial internal electron transfer from the ligands makes the central iron behave like a Fe(II) bound to semiquinone radicals (semi-dopaminequinone or semi-DAQ) (Fig. 1). Such a complex binds O₂ forming a ternary complex from which the electron transfer between oxygen and the ligands (DA) is greatly accelerated. Semi-DAQ is susceptible to oxidation by O₂ to produce H₂O₂ and dopaminequinone (DAQ) which can be further changed into leucodopachrome (LEUCO-DACHR) via an internal Michael-type electrophilic addition reaction. Dopachrome (DACHR, the oxidation product of LEUCO-DACHR) turns to neuromelanin finally.

In this paper, we investigate the formation of the ternary complexes of DA-Fe(III) with nitrilotriacetic acid (NTA), a tetradentate ligand [25]. The influence of the additional ligation by NTA on the redox potentials of DA and Fe(III) in the complex was studied by electrochemical techniques. The impact of additional ligation by NTA on the catalytic oxidation kinetics of DA was investigated with UV-vis spectrophotometer. The results revealed that NTA almost totally shut down the catalytic

oxidation of DA via the blockage of the oxygen access to the Fe(III) center. The variation in the kinetics was explained and correlated with the redox potential variation. The implication of the findings to the pathogenesis of PD was also discussed.

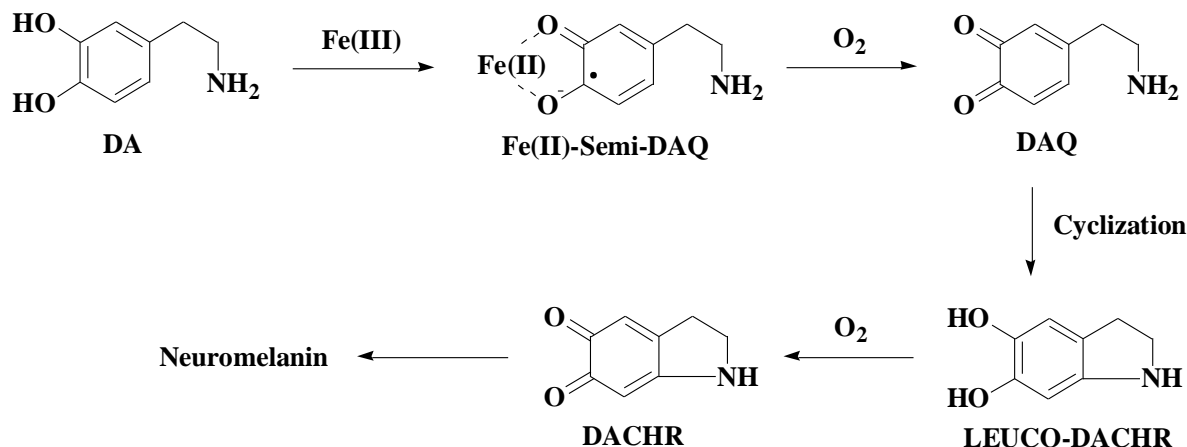


Figure 1. The proposed mechanism for the Fe(III)-promoted formation of neuromelanin.

2. EXPERIMENTAL

2.1 Chemicals and reagents

Dopamine hydrochloride was obtained from Aladdin reagent Inc. (Shanghai, China). Ferric nitrate nonahydrate ($\text{Fe}(\text{NO}_3)_3 \cdot 9\text{H}_2\text{O}$), sodium nitrate (NaNO_3), trifluoroacetic acid, 2-Amino-2-hydroxymethyl-propane-1,3-diol (Tris), acetonitrile, nitrilotriacetic acid and 2-[4-(2-hydroxyethyl)-1-piperazine]ethanesulfonic acid (HEPES) were of analytical grade and were used without further purification. The stock solution of 10 mM Fe(III) was prepared by dissolving an appropriate amount of $\text{Fe}(\text{NO}_3)_3 \cdot 9\text{H}_2\text{O}$ in 5 mM H_2SO_4 . The stock solution of 10 mM DA was prepared with deionized water before use. All aqueous solutions were prepared with deionized water treated with a Simplicity Plus Millipore purification system.

2.2 Electrochemical Measurements

The electrochemical measurements were performed on a CHI 411 electrochemical workstation in a homemade plastic three-electrode cell. The three-electrode system comprises a glassy carbon disk electrode with a diameter of 3 mm, a platinum wire auxiliary electrode, and a Ag/AgCl reference electrode. Prior to each measurement, the glassy carbon electrode was polished with diamond pastes down to 3 μm and then alumina pastes down to 0.3 μm . The HEPES buffer (50 mM, pH 7.2) containing 0.1 M NaNO_3 was used as the electrolyte solution. The electrochemical workstation and the three-electrode cell were housed in a nitrogen-purged glove box. In the anaerobic conditions, the O₂

content in the nitrogen-purged glove box was maintained at less than 1 μM , which was measured by a dissolved oxygen membrane electrode.

2.3 UV-vis spectroscopic measurements

UV-vis spectra were recorded with a Cary 100 Bio UV-vis spectrophotometer (Varian Inc., Palo Alto, CA). Optical measurements were conducted in Tris buffer (50 mM, pH 7.2) at 25 ± 1 °C. The kinetics of DA-Fe(III) and DA-Fe(III)-NTA under aerobic condition was followed spectrophotometrically at 570 and 610 nm, respectively, where the complex shows a maximum absorption from phenolate (π) \rightarrow Fe (III) ($d\pi^*$) ligand-to-metal charge transfer (LMCT) transition [10, 22].

3. RESULTS AND DISCUSSION

3.1 Formation of DA-Fe(III)-NTA ternary complex

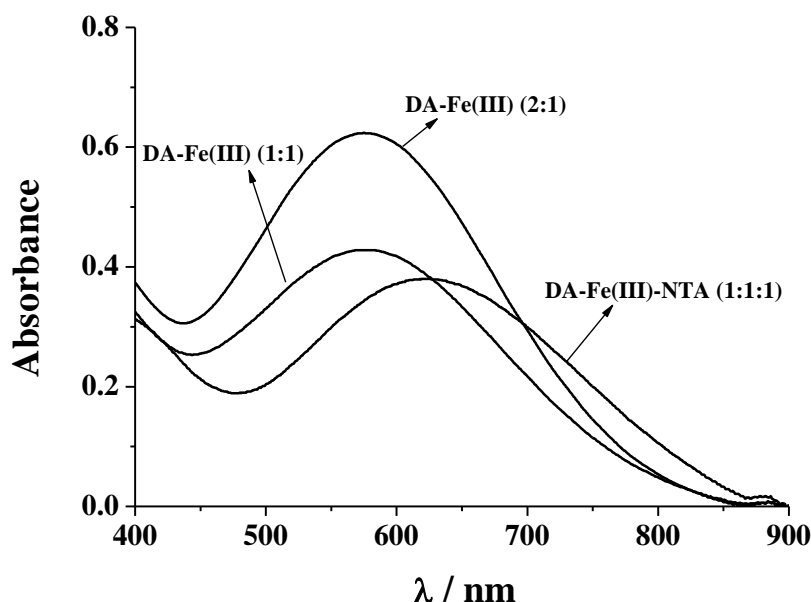


Figure 2. UV-vis spectrum of DA-Fe(III) and DA-Fe(III)-NTA. The concentration of Fe(III) and NTA were 250 μM .

Catecholatoiron(III) complex displays relatively intense absorption bands in the visible and near-IR regions, due to phenolate (π) \rightarrow Fe (III) ($d\pi^*$) LMCT transition and phenolate (σ) \rightarrow Fe (III) ($d_{x^2-y^2}/d_z^2$) LMCT transition [16, 26]. The DA-Fe(III) complex exhibits a characteristic absorption in UV-vis spectrum at around 570 nm corresponding to the LMCT transition [10, 27]. Usually a constituent group on the catechol ring or additional ligation to metal center by additional ligand will bring about absorption peak shift [15, 28, 29]. To validate the formation of ternary complex among DA, Fe(III) and NTA, we measured the UV-vis spectra of DA/Fe(III) mixture with and without NTA. As shown in Fig. 2, with the ratio of DA/Fe(III) of 2 in the absence of NTA, the characteristic peak at

570 was indicative of the formation of the DA-Fe(III) complex. It is generally suggested that Fe(III)(DA)₂ is the dominant form of complexes at neutral pH. Decreasing the ratio to 1:1 caused the characteristic peak size to be about halved, suggesting a decreased LMCT transition intensity. This result indicated that a complex with 1:1 stoichiometry is formed in this case. Interestingly, when a mixture with the ratio of 2:1:1 of DA/Fe(III)/NTA was measured, the characteristic catecholate-to-Fe(III) LMCT transition absorption peak shift to 610 nm and the peak size was also halved. The shift in the absorption peak position suggested that a new complex involving NTA was formed. The decrease in the peak size suggested that in the complex the DA moiety was decreased, which resulted in a decreased catecholate-Fe(III) LMCT transition. A point worth to mention is that increasing NTA further than 1 in the ratio did not alter the characteristic peak (data not shown). Taken together, the above observations clearly demonstrated that a stable ternary complex of 1:1:1 stoichiometric ratio among DA, Fe(III) and NTA was formed. Moreover, NTA replaced the second DA in Fe(III)(DA)₂ complex, but did not replace all the DA in the complex. So the binding affinity of NTA to DA-Fe(III) was estimated to be in the range between the binding affinity of first DA and second DA.

3.2 Voltammetric responses of DA-Fe(III) and DA-Fe(III)-NTA

In order to probe how the ligation of NTA affects the iron catalytic oxidation of DA by oxygen, we conducted the electrochemical investigation of the DA-Fe(III) binary complex and the DA-Fe(III)-NTA ternary complex. Fig. 3 shows the CVs of free DA and the complexes of DA-Fe(III) and DA-Fe-NTA. Two couples of redox peaks in Fig. 3A corresponding to the redox reactions of DA/DAQ and LEUCO-DACHR/DACHR were obtained. DA was first oxidized to DAQ at 0.251 V, which was followed by a quick cyclization process to LEUCO-DACHR via an internal Michael addition reaction, as evidenced by the much smaller reduction peak at 0.158 V. The resulting LEUCO-DACHR was further oxidized to DACHR at potentials positive than -0.182 V. Thus, the electrode reaction is characteristic of an ECE mechanism (electron transfer-chemical reaction-electron transfer). The featureless voltammetric curve recorded between 0.05 V and -0.8 V (black curve in Fig. 3D) further indicated that the oxidation of DA is a crucial step for the formation of DACHR. However, after binding to Fe(III), the oxidation peak potential of DA shifted to 0.353 V (Fig. 3B). A positive potential shift for the oxidation of DA in the complex implied a declined electron density on the DA, and partial electron transfer from DA to iron center. Thermodynamically, the positive shift indicated that the strong affinity of catecholate to Fe(III) significantly stabilized the DA oxidation level. Moreover, in contrast to the CV of DA in the absence of Fe(III) (Fig. 3A), the redox waves with $E_{p_c} = -0.392$ V and $E_{p_a} = -0.185$ V (red curve in Fig. 3D) should be attributed to the reduction/reoxidation of the iron redox center in the DA-Fe(III) complex. The value of Fe(III)/Fe(II) redox potential is similar to that of Fe(III)-catecholate complex [21, 30]. As expected, the redox potential of iron is shifted in an opposite direction to a more negative potential (a median peak potential of -0.287 V). The potential is lower than that of free Fe(III)/Fe(II) (0.575 V vs. Ag/AgCl) [31]. A negative shift in the iron redox potential indicates an increased Lewis acidity of the iron center in the complex. Further ligation by any additional ligands maybe alter the redox potential of both Fe(III) center and cataecholate ligands.

Indeed, as shown in the Fig. 3C, the additional ligation by NTA shifted positively the oxidation potential of DA to 0.440 V in the complex. The shift of redox potential of DA in the presence of Fe(III) or Fe(III)-NTA was also confirmed by DPVs (Fig. 3F). Meanwhile, the redox behavior of Fe(III) center was altered with the reduction peak negatively shifted to -0.514 V and the oxidation peak shifted to above 0.050 V, demonstrating that the additional ligation by NTA enforced the electron donation by DA to the iron center, or increases the Lewis acidity of metal center.

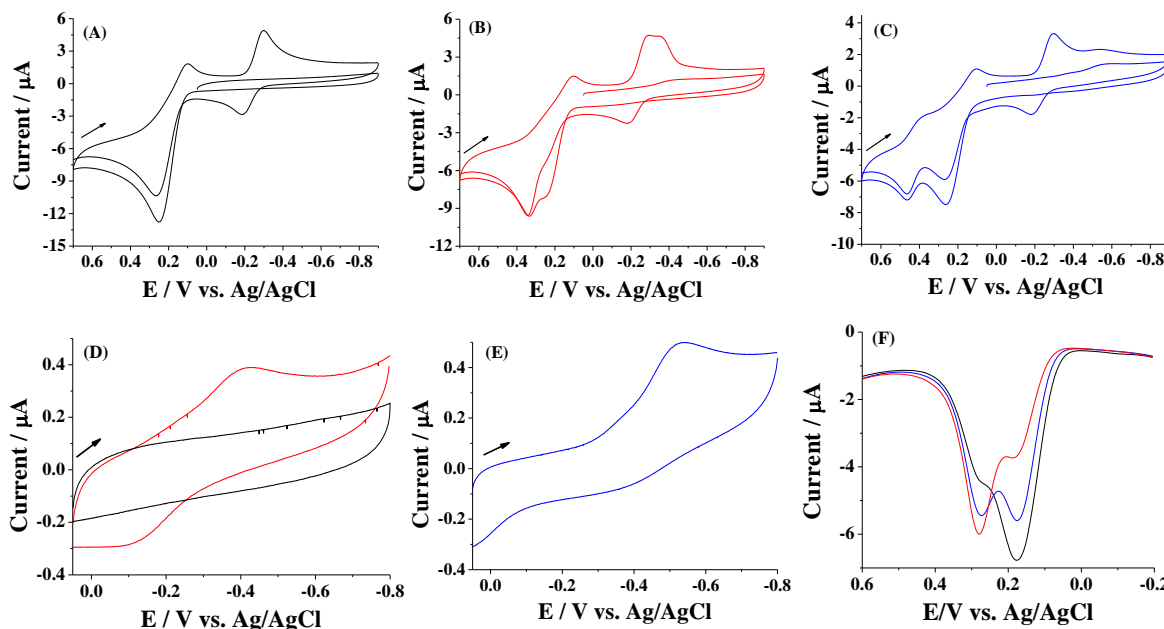


Figure 3. (A) Cyclic voltammograms (CVs) of DA (A), DA-Fe(III) (B) and DA-Fe(III)-NTA (C). The scan rate was 50 mV s^{-1} . Panels D and E show the CVs of DA (black curve), DA-Fe(III) (red curve) and DA-Fe(III)-NTA (blue curve) at the potential range of $0.05 \text{ V} \sim -0.8 \text{ V}$ with a scan rate of 10 mV s^{-1} . Panel F shows the differential pulse voltammograms (DPVs) of DA (black curve), DA-Fe(III) (red curve) and DA-Fe(III)-NTA (blue curve) at the potential range of $-0.2 \text{ V} \sim 0.6 \text{ V}$. The concentration of DA, Fe(III) and NTA are 500, 250 and 250 μM , respectively. The arrow indicates the scan direction.

3.3 Kinetic analysis of DA-Fe(III) and DA-Fe(III)-NTA

As depicted in Fig. 2, DA-Fe(III) and DA-Fe(III)-NTA exhibited a maximum absorption at 570 nm and 610 nm, respectively. The stability of these complexes under aerobic condition was therefore examined by determining the absorbance changes at 570 nm and 610 nm, respectively. We found that DA-Fe(III) complex increased slightly with time and then decreased from 240 min. The increase before 240 min in absorbance can be attributed to the formation of DAQ and DACHR, which also show a absorption at 570 nm although their maximum absorptions are positioned at 395 and 475 nm, respectively [32]. The decrease in absorbance should be caused by the formation of neuromelanin and the follow-up sequestration of Fe(III) by NM to form the precipitates. Actually, the black precipitate was also observed by eyes after 5h. However, in the presence of NTA, much smaller change in the

absorbance of DA-Fe(III)-NTA was obtained. Further results also indicated that the formation of NM could be inhibited by NTA for two days experiment.

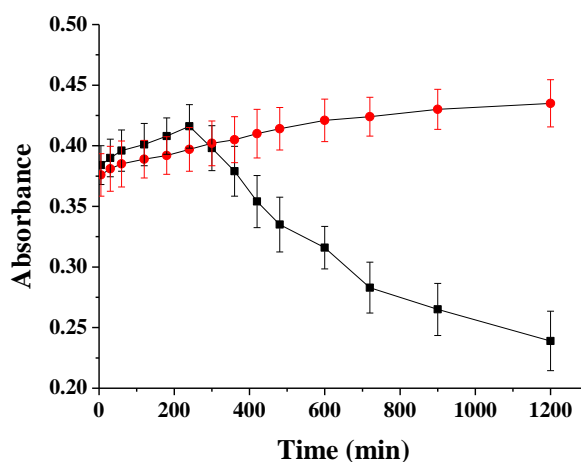


Figure 4. The kinetics of DA-Fe(III) (black) and DA-Fe(III)-NTA (red) under aerobic condition. The concentrations of DA, Fe(III) and NTA were 250 μ M.

3.4 H_2O_2 generation

As mentioned in introduction, H_2O_2 can be produced from the oxidation of Fe(III)-catalyzed DA oxidation. In this work, the amount of H_2O_2 generated from the DA/Fe(III) mixture was determined with the commercial wired HRP/polymer electrode prepared following the user manual (BASi) [33]. As shown in Fig. 5, little H_2O_2 was found in the solution of DA alone, which may be attributed to the auto-oxidation of DA in air-saturated solution. In the DA-Fe(III) system, the amount of H_2O_2 increased with incubation time, indicating that Fe(III) promoted the oxidation of DA and the formation of H_2O_2 . However, with the addition of NTA, the amount of H_2O_2 is smaller than that in the absence of NTA. Therefore, it is reasonable to suggest that NTA can inhibit the Fe(III)-catalyzed DA oxidation and suppress the formation of H_2O_2 .

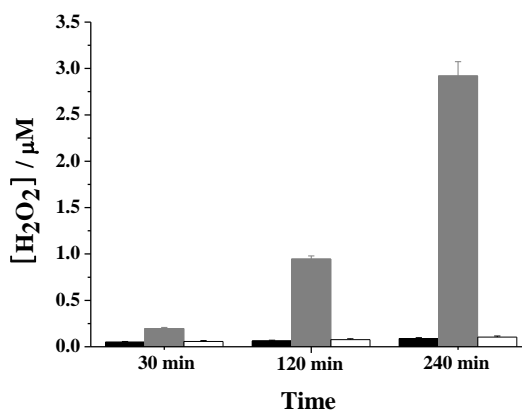


Figure 5. Concentration of H_2O_2 generated from the solutions of DA alone (black bars), DA and Fe(III) (gray bars) and DA, Fe(III) and NTA (white bars) for different incubation periods (30, 120, and 240 min). The concentrations of DA, Fe(III) and NTA were 250 μ M.

3.5 Mechanism of Fe(III)-mediated DA oxidation and the effect of NTA

The experimental results demonstrated that DA, Fe(III) and NTA form a stable ternary complex and the additional coordination of NTA totally annihilates the Fe(III) catalytic effect in DA oxidation by O₂. Of great interest are the facts that the binding of NTA reverses the Fe(III) catalytic effect in DA oxidation and the mechanism behind such a drastic inhibitory effect. In particular, such an inhibitory effect is inconsistent with the prediction based the common rules well documented for the study of model complexes of dioxygenase [14, 34]. It has been suggested that the increased covalency of the Fe(III)-catecholate bond or the Lewis acidity of Fe(III) would increase the catalytic activity of the complex toward the catalytic oxidation of catechols involved [14, 34]. Inconsistent with this rule is that despite the increase in the covalency of Fe(III)-catecholate bond and the Lewis acidity of Fe(III) by NTA additional coordination, the catalytic oxidation activity failed to increase. A credible explanation to such inconsistency is that the key step in the Fe(III) catalyzed oxidation of DA is blocked due to the additional coordination by NTA. The proposed mechanism of Fe(III)-catalytic DA oxidation is described in Fig. 6. Instead of outer-sphere alternate electron transfer catalytic mechanism, the reaction undergoes an inner sphere electron transfer process. Specifically, Fe(III) quickly binds DA forming DA-Fe(III) complexes. At neutral pH, Fe(III) associates one or two DA molecules depending on the availability of DA. Both complexes have open shell structure with unsaturated coordination sites on the Fe(III) center. The activation of oxidation starts with the access of O₂ to the empty or weakly occupied coordination sites. The partial electron transfer from DA to Fe(III) center makes the center possess Fe(II) characteristics and increases O₂ propensity for the center. As a result, an intermediate, the O₂-Fe(III)-DA, is formed. Through the metal center bridge, two electrons from DA eventually transfer to O₂. Then, the intermediate dissociates into hydrogen peroxide, DAQ and Fe(III). NTA, a tetradentate ligand, will replace a DA molecule in the complex of Fe(III)(DA)₂, resulting in the formation of a close shell ternary complex of DA-Fe(III)-NTA. In the ternary complex all the coordination sites of the iron center are occupied, which leaves no room for the O₂ to access. Despite the lack of structural data of the ternary complex, the credence of the account is further provided by the fact that similar inhibitory effect was found when another tetradentate ligand known to form close shell ternary complex with Fe(III) and catechols was used [35]. Taken together, the reactive iron and excess cytosolic DA maybe play a positive role in DA neuron dysfunction by promoting the generation of ROS. Because the formation of ternary complex among DA, Fe(III) and O₂ is the prerequisite for the catalytic reaction, any other ligand which can form ternary complex with DA-Fe(III) complex should also block or impede O₂ from accessing the iron center. In the biological milieu, there exist a number of small ligands. Given the availability of DA, Fe(III) and iron ligation in/at the dopaminergic cells, it is very likely that a ternary complex is present in/or at a normal dopaminergic cell. Therefore, our finding may provide a significant insight into how DA, a potentially toxic and highly functional molecule, is handled in a normal neuron.

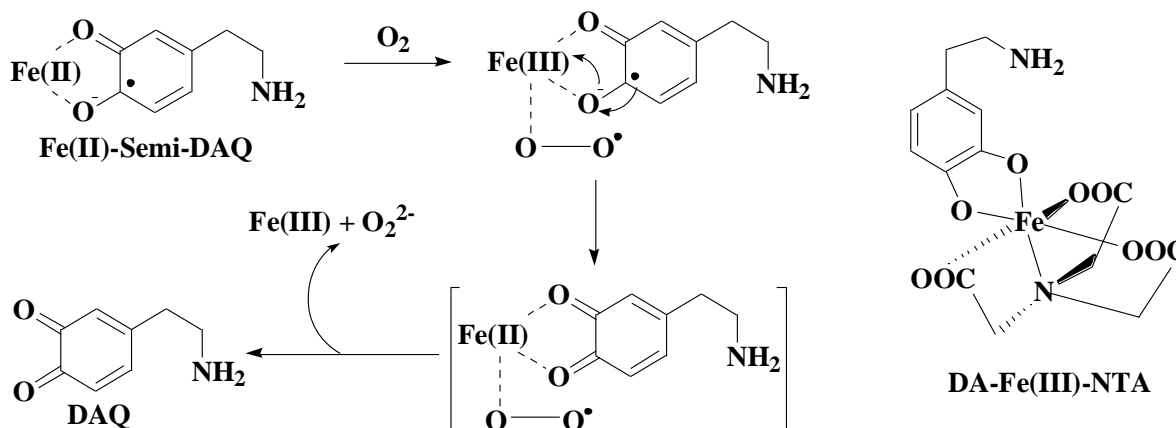


Figure 6. the proposed mechanism of iron catalyzed DA oxidation by O₂ and the speculated structure of the DA-Fe(III)-NTA complex.

4. CONCLUSION

The DA-Fe(III)-NTA ternary complex was identified, and its spectroscopic and redox properties were studied in this work. In comparison with DA-Fe(III) complex, the LMCT band of the ternary complex shifted to a longer wavelength, the redox potential of DA in the complex is positively shifted and that of Fe(III) center is negatively shifted. Remarkably, the additional binding by NTA totally annihilates Fe(III) catalytic activity in the catalytic oxidation of DA by O₂. The finding may have a significant biological implication in understanding the pathogenesis of PD and developing novel drugs.

ACKNOWLEDGEMENTS

This work was supported by the Fund of Department of Science and Technology Department in Henan (KJT142102310462), the Youth Research Foundation in Pingdingshan University (20120015) and the High-Level Personnel Fund in Pingdingshan University (1011014/G).

References

1. D. J. Moore, A. B. West, V. L. Dawson and T. M. Dawson, *Annu. Rev. Neurosci.*, 28 (2005) 57.
2. K. A. Malkus, E. Tsika and H. Ischiropoulos, *Mol. Neurodegener.*, 4 (2009) 24.
3. L. Liu, J. Du, S. Li, B. Yuan, H. Han, M. Jing and N. Xia, *Biosens. Bioelectron.*, 41 (2013) 730.
4. J. D. Erickson, L. E. Eiden and B. J. Hoffman, *Proc. Natl. Acad. Sci. USA*, 89 (1992) 10993.
5. Y. Liu, D. Peter, A. Roghani, S. Schuldiner, G. G. Privé, D. Eisenberg, N. Brecha and R. H. Edwards, *Cell* 70 (1992) 539.
6. J. D. Elsworth and R. H. Roth, *Exp. Neurol.*, 144 (1997) 4.
7. D. Sulzer and L. Zecca, *Neurotox. Res.*, 1 (2000) 181.
8. L. Zecca, A. Stroppolo, A. Gatti, D. Tampellini, M. Toscani, M. Gallorini, G. Giaveri, P. Arosio, P. Santambrogio, R. G. Fariello, E. Karatekin, M. H. Kleinman, N. Turro, O. Hornykiewicz and F. A. Zucca, *Proc. Natl. Acad. Sci. USA*, 101 (2004) 9843.

9. I. Irwin and J. W. Langston. *Endogenous toxins as potential etiologic agents in Parkinson's disease*. Marcel Dekker, New York (1995).
10. A. Pezzella, M. d'Ischia, A. Napolitano, G. Misuraca and G. Prota, *J. Med. Chem.*, 40 (1997) 2211.
11. A. T. McKie, D. Barrow, G. O. Latunde-Dada, A. Rolfs, G. Sager, E. Mudaly, M. Mudaly, C. Richardson, D. Barlow, A. Bomford, T. J. Peters, K. B. Raja, S. Shirali, M. A. Hediger, F. Farzaneh and R. J. Simpson, *Science*, 291 (2001) 1755.
12. M. E. Götz, K. Double, M. Gerlach, M. B. Youdim and P. Riederer, *Ann. N. Y. Acad. Sci.*, 1012 (2004) 193.
13. R. Ortega, P. Cloetens, G. Devès, A. Carmona and S. Bohic, *PLoS ONE*, 2 (2007) e925.
14. M. M. Abu-Omar, A. Loaiza and N. Hontzeas, *Chem. Rev.*, 105 (2005) 2227.
15. S. Arreguin, P. Nelson, S. Padway, M. Shirazi and C. Pierpont, *J. Inorg. Biochem.*, 103 (2009) 87.
16. L. K. Charkoudian and K. J. Franz, *Inorg. Chem.*, 45 (2006) 3657.
17. W. R. Harris, C. J. Carrano, S. R. Cooper, S. R. Sofen, A. E. Avdeef, J. V. McArdle and K. N. Raymond, *J. Am. Chem. Soc.*, 101 (1979) 6097.
18. R. Mayilmurugan, K. Visvaganesan, E. Suresh and M. Palaniandavar, *Inorg. Chem.*, 48 (2009) 8771.
19. M. Palaniandavar, M. Velusamy and R. Mayilmurugan, *J. Chem. Sci.*, 118 (2006) 601.
20. M. Velusamy, R. Mayilmurugan and M. Palaniandavar, *Inorg. Chem.*, 43 (2004) 6284.
21. R. Viswanathan, M. Palaniandavar, T. Balasubramanian and T. P. Muthiah, *Inorg. Chem.*, 37 (1998) 2943.
22. D. Zirong, S. Bhattacharya, J. K. McCusker, P. M. Hagen, D. N. Hendrickson and C. G. Pierpont, *Inorg. Chem.*, 31 (1992) 870.
23. W. Linert, E. Herlinger, R. F. Jameson, E. Kienzl, K. Jellinger and M. B. H. Youdim, *Biochim. Biophys. Acta.*, 1316 (1996) 160.
24. W. Linert and G. N. L. Jameson, *J. Inorg. Biochem.*, 79 (2000) 319.
25. V. Ranc, Z. Markova, M. Hajduch, R. Pucek, L. Kvitek, J. Kaslik, K. Safarova and R. Zboril, *Anal. Chem.*, 86 (2014) 2939.
26. L. Liu, S. Li, L. Liu, D. Deng and N. Xia, *Analyst*, 137 (2012) 3794.
27. J. Porter, S. Arreguin and C. G. Pierpont, *Inorg. Chim. Acta*, 363 (2010) 2800.
28. M. Kaya and M. Volkan, *Anal. Chem.*, 84 (2012) 7729.
29. L. Liu, G. Wang, Q. Feng, Y. Xing, H. Han and M. Jing, *Int. J. Electrochem. Sci.*, 8 (2013) 3814.
30. N. Cheraiti, M. E. Brik, L. Bricard, B. Keita, L. Nadjo and A. Gaudemer, *Bioorg. Med. Chem. Lett.*, 9 (1999) 2309.
31. A. J. Bard and L. R. Faulkner. *Electrochemical Methods. Fundamentals and Applications*. John Wiley and Sons, New York (2001).
32. M. Bisaglia, S. Mammi and L. Bubacco, *J. Biol. Chem.*, 282 (2007) 15597.
33. <http://www.basinc.com/products/ec/perox.php> (Accessed March 8, 2014).
34. M. Costas, M. P. Mehn, M. P. Jensen and L. Que Jr., *Chem. Rev.*, 104 (2004) 939.
35. L. Que, Jr., R. C. Kolanczyk and L. S. White, *J. Am. Chem. Soc.*, 109 (1987) 5373.